Journal of Medical Systems (2019) 43: 173
https://doi.org/10.1007/s10916-019-1313-6

PATIENT FACING SYSTEMS

Distinguising Proof of Diabetic Retinopathy Detection by Hybrid Approaches in Two Dimensional Retinal Fundus Images

Karkuzhali S[1] · Manimegalai D[2]

Received: 8 March 2019 / Accepted: 25 April 2019 / Published online: 8 May 2019

Abstract

Diabetes is characterized by constant high level of blood glucose. The human body needs to maintain insulin at very constrict range. The patients who are all affected by diabetes for a long time affected by eye disease called Diabetic Retinopathy (DR). The retinal landmarks namely Optic disc is predicted and masked to decrease the false positive in the exudates detection. The abnormalities like Exudates, Microaneurysms and Hemorrhages are segmented to classify the various stages of DR. The proposed approach is employed to separate the landmarks of retina and lesions of retina for the classification of stages of DR. The segmentation algorithms like Gabor double-sided hysteresis thresholding, maximum intensity variation, inverse surface adaptive thresholding, multi-agent approach and toboggan segmentation are used to detect and segment BVs, ODs, EXs, MAs and HAs. The feature vector formation and machine learning algorithm used to classify the various stages of DR are evaluated using images available in various retinal databases, and their performance measures are presented in this paper.

Keywords Optic Disc · Diabetic Retinopathy · Hemorrhages · Blood Vessels · Microaneurysms · Image Processing

Introduction

The diabetes is a chronic condition associated with high blood sugar levels. All patients who have been diagnosed with type-I Diabetes mellitus (DBM) or non insulin-dependent type-II diabetes mellitus are at the hazard of evolving DR. In type-I Diabetes mellitus and non insulin-dependent type-II diabetes mellitus, the human body fails to generate insulin properly or cells fail to utilize insulin properly. The early and proper diabetes treatment is cost efficient [1]. The consequence of untreated diabetes may lead to progression of DR. DR is an ocular manifestation of diabetes, and DBM are at the hazard of loss of vision due to Diabetic Retinopathy. DR is a growing gradual capillary bed loss in the retina and loss of supply of blood to active retinal photoreceptors. DR is characterized by adverse changes in BVs leading to vision loss without any symptoms. The loss of blood supply in addition to nutrients such as glucose to retinal cell die and vision loss is due to DR. The slaughter of capillary bed and tissue blood supply to kidney, heart, and peripheral nerves due to diabetes may lead to renal failure, cardiac disease and neuropathy [2].

Diabetic Retinopathy is widely categorized into 2 stages, and they are PDR (proliferative diabetic retinopathy) and NPDR (non-proliferative diabetic retinopathy). NPDR is a treatable stage, also known as background DR, whereas the PDR is the advanced diabetic retinopathy stage. NPDR exists due to diabetes which damages the retinal BVs causing blood leakage, lipid and protein on the retina surface. The swollen and wet condition is because of this leakage that reduces the functionality of retina. NPDR may contain physical signs like MAs, HAs, EXs and CWSs. NPDR is divided into severe, mild and moderate stages based on the presence of the amount of these lesions. DR is commonly classified into the following stages.

a. Mild NPDR: Near the beginning stage of Mild non-proliferative DR has the symptoms like presence of MA's which is small circular region like swelling in retinal blood vessels.

This article is part of the Topical Collection on *Patient Facing Systems*

✉ Karkuzhali S
vijikarkuzhali@gmail.com

Manimegalai D
megalai_nec@yahoo.co.in

[1] Department of Computer Science and Engineering, Kalasalingam Academy of Research and Education (Deemed to be University), Srivilliputtur, Tamilnadu, India

[2] Department of Information Technology, National Engineering College, Kovilpatti, Tamilnadu, India

b. Moderate non-proliferative diabetic retinopathy: At this stage, MAs, HAs, EXs and CWSs will be observed together or appear independently. The other abnormalities like venous bleeding, Intra-Retinal Micro vascular Abnormality (IRMA) may be present in the retina.
c. Severe NPDR: This is the misguided way of attempting to send blood supply to central region of retina. In this stage, severe retinal HAs in four quadrants or venous bleeding in two quadrants or IRMA in one quadrant are present. Any two conditions that get satisfied in 4:2:1 ratio indicates very severe stage [3].
d. PDR: At this highly developed stage, the new BVs are abnormal and fragile due to lack of oxygen, and the leakage or bleeding occur and give rise to HAs. The leakage in vitreous gel creates vitreous HAs. Figure 1 shows the stages of DR.

DR is diagnosed and classified by ophthalmologist, optometrists and eye care professionals to determine whether the patients are in need of follow up or laser treatment. The screening of DR is performed using examination methods like slit lamp biomicroscopy, direct or indirect ophthalmoscopy and dilated or nondilated digital fundus photography. The most common method used is by examining digital fundus photography [4]. The manual screening process imposes a heavy workload on the ophthalmologists who have to evaluate a huge amount of fundus images every day. The other barriers to achieve

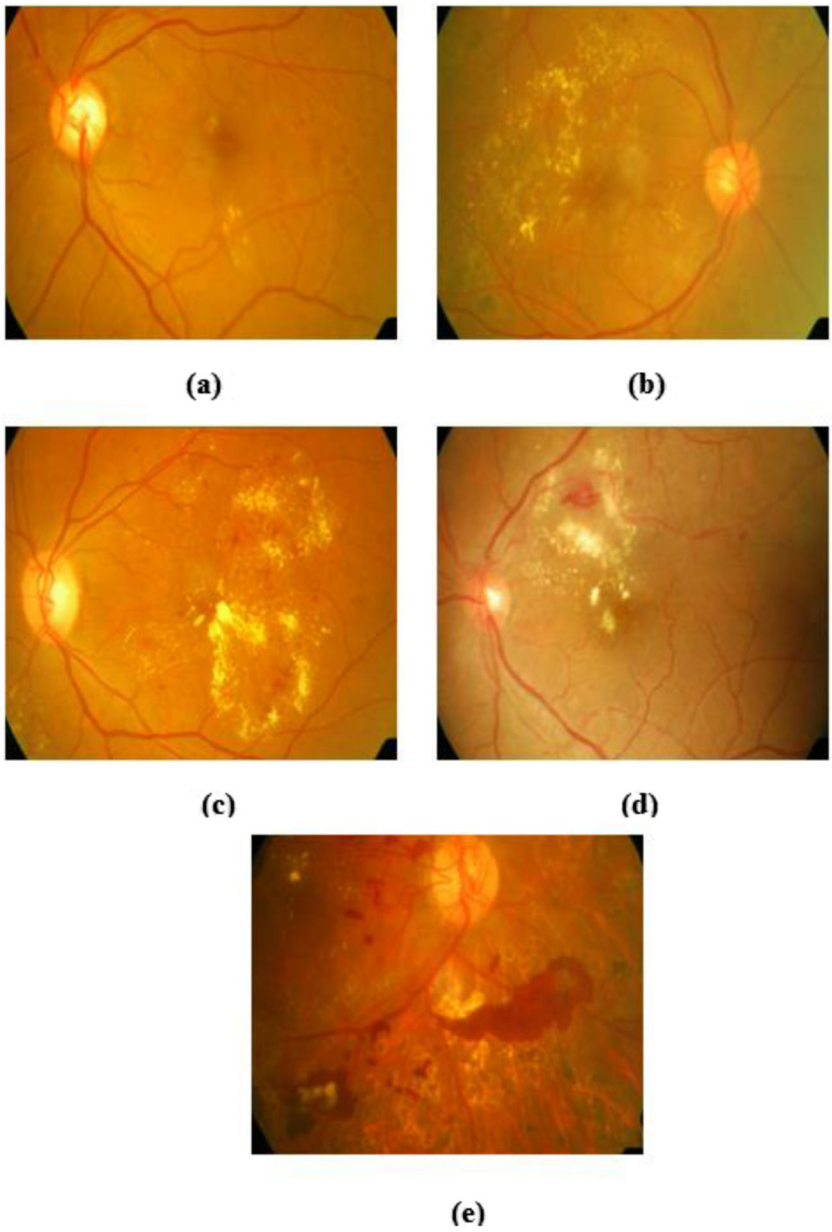

Fig. 1 The stages of DR a) Mild Non-Proliferative Diabetic Retinopathy b) Moderate Non-Proliferative Diabetic Retinopathy c) Severe Non-Proliferative Diabetic Retinopathy d) Very Severe Non-Proliferative Diabetic Retinopathy e) Proliferative Diabetic Retinopathy. (Source: Images collected from Bejan singh eye hospital, Nagerkoil)

recommended screening system are growing number of retinal disease affected patients and cost of current hospital-based system. The growth of a computer aided system of screening with image processing techniques to diagnose Diabetic Retinopathy and support is the essential solution to this issue. Table 1 shows the various stages of DR. The international clinical severity scale for detection of DR is summarized in Table 2 and Table 3.

(Source: Saleh et al. 2012)

Where MAs-micro aneurysms, CWs-cotton wool spots, HAs- hemorrhage, IRMA-intra retinal micro vascular abnormality, EXs-exudates, VB-venous bleeding, FPD-fibrous proliferation disc, VH-vitreous hemorrhage, PRH-pre-retinal hemorrhage.

The OD is detected using Fuzzy C means(FCM) followed by maximum intensity variation algorithm, and BVs are segmented by means of Gabor double-sided hysteresis thresholding in fundus images. EX, MA and HA segmentations are carried out by an inverse surface adaptive thresholding, a multi-agent approach and toboggan segmentation, and the effectiveness of the algorithm is compared with the existing algorithms mentioned in the literature. In this proposed work, out of fifty five, fifteen statistically significant ($p < 0.0001$) features are extracted and used for NB, SVM-RBF to classify images as normal/abnormal. Again with the feature vector, pattern recognition neural networks (PRNN), RBFEF, RBFFN classifiers are used to classify all the stages of DR.

Literature Survey

The increasing number of diabetic patients has highly motivated the researchers in developing automated tools to screening DR. The literatures related to segmentation of BVs, segmentation of EXs, detection of MAs, identification of HAs and classification of DR are discussed below.

In recent years, the progressively increasing number of diabetic patients has inspired researchers to develop methodologies and diagnostic tools to screening DR. Algorithms described in the literature for the detection and classification of DR are discussed below.

Acharya et al. (2016) have proposed two dimensional integrated index and empirical mode decomposition and integrated index to detect the morphological changes in fundus images. The essential features are extracted and ranked to feed as input into SVM-RBF classifier, which is employed to classify abnormal and normal images of retina. The performance measures like an SE, SPE and ACC of the system are 88.63%, 86.25% and 91% respectively [5]. Mahendran et al. (2015) have developed a score computation technique to detect EXs. The GLCM (Gray-Level Co-occurrence Matrix) is extracted and given as input to SVM and PNN classifiers. The evaluation of this algorithm is done by the classification ACC of 98% and 95% for Support Vector Machine and Probabilistic Neural Network classifier respectively [6].

Imani et al. (2015) have proposed Morphological Component Analysis(MCA), statistical feature extraction and SVM to discriminate and distinguish the normal and pathological retinal structures. This methodology has achieved an Sensitivity(SE) and Specificity(SPE) of 84.44% and 90.73% respectively [7]. Figueiredo et al. (2015) have proposed wavelet multi-scale analysis Hessian matrix and cartoon texture decomposition to detect MAs, HAs and EXs. The contextual features are retrieved and provided to binary classifier for the normal and abnormal images classification. This method has yielded an SE of 95-100% and SPE of 70% respectively [8].

Mookiah et al. (2013) have proposed a method based on evolutionary algorithm to classify the stages of DR. The EXs and BVs are segmented using simple thresholding and 2D Gabor matched filter technique. The area, node point count, texture, entropy features are extracted and statistical analysis is performed on the features. The PSO (Particle Swarm Optimization) and GA (Genetic Algorithm) are used to optimize the features, and PNN classifier is used to categorize images into normal, proliferative diabetic retinopathy and non proliferative diabetic.retinopathy. This methodology has yielded an SE, SPE and ACC of 96.27%, 96.08% and 96.15% respectively [9].

Table 1 Various stages of DR

Stages of DR	Description
Non proliferative diabetic retinopathy	Early NPDR
	Microaneurysms
	Dot, blot or flame Hemorrhages
	Late NPDR
	Exudates
	Cotton wool spots
	Intraretinal micro-vascular abnormality
	Venous bleeding
Proliferative diabetic retinopathy	Growth of abnormal blood vessels
	Pre-retinal/vitreous hemorrhage

Table 2 International clinical severity scale for detection of DR

Severity level	Finding observable with dilated ophthalmoscope
No apparent retinopathy	No abnormalities
Mild NPDR	MAs only
Moderate NPDR	HAs, MAs, CWS, EX, IRMA but less than severe NPDR
Severe NPDR	HAs and/or MAs in all four quadrants, or venous bleeding in two or more quadrants or IRMA in at least one quadrant
Very severe NPDR	Any two of the changes in severe NPDR
PDR	One or more of the following: neovascularization, vitreous/pre-retinal HMs

Kumar et al. (2012) have proposed the Gabor filter, thresholding and morphological operation to segment abnormalities. The parameters of OD, thickness of BVs and vein diameter are retrieved and fed as input to Support Vector Machine classifier(SVM) to achieve an ACC of 97.47%. [10] Madheswaran et al. (2012) have used thresholding and morphological operation to segment bright and dark lesions. The bright and dark lesions are differentiated by SVM classifier with an ACC of 98.19% and 97.51% respectively [11].

The detailed review concludes that developing and implementing of image processing algorithms for segmenting the anatomical and pathological features are the ongoing challenge to develop the screening system of DR. The above-mentioned challenges give rise to the need of efficient segmentation methods with less computational complexity for segmenting the features in retinal images. Tables 4,5,6,7, 8 shows the comparative analysis of segmentation of BV, OD, EX, MAs and HAs with literature-reviewed methods.

Database Used

The images of retina are downloaded from the database of DRIVE (http://www.isi.uu.nl/Research/Databases/DRIVE/). A set of 40 fundus images with 33 normal images and 7 DR affected images are available. It is acquired by Canon CR5 non-mydriatic 3CCD camera with 45° FOV. Every image is seized using 8 bits/color plane at 565 × 584 pixels [12].

Table 3 Early Treatment of Diabetic retinopathy Study severity scale for diagnosis of DR

Grade	Severity level	Description
10	No DR	–
20	MAs only	MA
35	Mild NPDR	CWS,HMs or IRMA or EX or CWS
47	Moderate NPDR	HAs/MAs or IRMA
53	Severe NPDR	HAs/MAs or IRMA or VB
61	Mild PDR	FPD
71	High risk PDR	VH or PRH or VB
81	Advance PDR	–

A set of 81 fundus photographs with 31 normal and 50 abnormal images from publicly available database of STARE (http:// http://cecas.clemson. edu/~ahoover/stare/) has been used, which are seized using TRV-50 fundus camera of Topcon. The images are seized using 24 bits/ pixel at 605 × 700 pixels with a 35° FOV [13]. A set of 1200 images consisting of 546 normal images and 654 abnormal images was downloaded from http://messidor.crihan.fr. and are captured using 3CCD camera color video on a TRC NW6 Topcon non-mydriatic retinography. Then the images are captured using 8 bits/plane at 2240 × 1488, 2304 × 1536 or 1440 × 960 pixels with a 45°FOV [14].

DIARETDB0 data set consisting of 130 images with 20 normal images and 110 DR affected images with unknown camera settings available in http://it.lut.fi/project/imageret/diaretdb0/ is used. The images are captured at 1500 × 1152 pixels with 50° FOV [15]. DIARETDB1 data set consisting of 89 images with 5 normal images and 84 DR affected images with various camera settings as available in http://it.lut.fi/project/imageret/diaretdb1/ is chosen. The images are captured at 1500 × 1152 pixels with 50° FOV [16]. A set of 100 DR affected retinal images was obtained with specific digitized fundus camera with a laser scanner film [Modem 3000, Zeiss Stratus OCT] in Bejan Singh Eye Hospital, Nagarcoil. The images are obtained with 2240 × 1488 pixels and saved in the file format of jpeg. The below table shows the summary of different sets of data (Table 9) [12–16].

Proposed Method

The OD is detected using FCM followed by maximum intensity variation algorithm, and BVs are segmented by means of Gabor double-sided hysteresis thresholding in fundus images. EX, MA and HA segmentations are carried out by an inverse surface adaptive thresholding, a multi-agent approach and toboggan segmentation, and the effectiveness of algorithm is evaluated with existing algorithms mentioned in the literature. In this proposed work, out of fifty five, fifteen significant statistically ($p < 0.0001$) features are extracted and employed for NB, SVM-RBF to classify images as normal/abnormal. Again with the feature vector, pattern recognition neural networks (PRNN), RBFEF, RBFFN classifiers are used to classify all the stages of DR. Fig. 2 shows methodology for CAD of DR.

Table 4 Comparison of retinal BV segmentation algorithm with literature-reviewed methods

Author name	Year	Algorithm	Database	No of images	SE (%)	SPE (%)	ACC (%)	Computation time(s)
Aslani et al.	2016	Hybrid feature vector formation	DRIVE	40	75.45	98.01	95.13	60
		Random forest classifier	STARE	20	75.56	98.37	96.05	
Christodoulidis et al.	2016	Multi scale tensor voting approach	Erlangen	45	85.06	95.82	94.79	1200
Kar et al.	2016	Matched filtering integrated with curvelet transform and kernel based fuzzy c means	DRIVE	40	75.48	97.92	96.16	730.85
			STARE	20	75.63	97.43	97.35	
			DIARETDB1	89				
Geetha ramani et al.	2016	Gabor filtering, half wave rectification, k-means clustering	DRIVE	40	70.79	97.78	95.36	NA
Singh et al.	2016	Gumbel probability distribution function based matched filter	DRIVE	40	75.94	97.08	95.22	135.6
			STARE	20	79.39	93.60	92.70	144
Kar et al.	2016	Band pass filter and fuzzy conditional entropy	DRIVE	40	76.32	98.01	96.28	148.48
			STARE	20	72.82	93.38	96.16	
Kovacs et al.	2016	Template matching	DRIVE	40	72.70	98.77	96.48	225
		Contour reconstruction	STARE	20	76.65	98.79	97.11	
Roychowdhury et al.	2015	Gaussian mixture model	DRIVE	40	72.5	98.3	95.2	3.1
			STARE	20	77.2	97.3	95.15	6.7
			CHASE_DB1	28	72.01	98.24	95.3	11.7
Imani et al.	2015	Morphological Component analysis, Shearlet transform	DRIVE	40	75.24	97.53	95.23	NA
			STARE	20	75.02	97.45	95.90	
Proposed method		Gabor double-sided hysteris thresholding	STARE	81	89.08	90.32	98.19	49.92 ms

Table 5 Comparison of OD localization algorithm with literature-reviewed methods

Author name	Year	Algorithm	Database	No of images	Success rate (%)	Computation time(s)
Xiong et al.	2016	Pathological changes extraction	DRIVE	40	100	NA
		ROI detection	STARE	81	95.8	
		Candidate pixel detection	DIARETDB0	130	99.2	
		Confidence score calculation	DIARETDB1	89	97.8	
Zhang et al.	2016	Vessel distribution characteristics (local vessel density, compactness, and uniformity) and global vessel directional characteristics	STARE	81	93.8-99.7	3.4-11.5
Soares et al.	2016	Cumulative sum field	STARE	81	98.77	12.02
		Modified corner detector Morphological operators	DRIVE	40	100	9.40
		Vessel convergence algorithm (High vascular convergence, high intensity value)	DIARETDB0	130	98.46	20.07
			DIARETDB1	89	98.88	20.07
			MESIDOR	1200	99.25	18.64
			ROC	100	99	20.94
			E-OPHTHA-EX	82	98.78	21.95
			HRF	45	100	23.65
Harangi et al.	2015	Combination of probability models	DIARETDB0	130	98.46	250 ms
		Single majority voting rule	DIARETDB1 DRIVE	89	98.88	
		Spatial weighted graph	MESIDOR	40	100	
				1200	98.33	
Marin et al.	2015	Automatic thresholding	MESSIDOR	1200	99.75	5.425
		Iterative opening-closing morphological operation	MESSIDOR2	1748	99.72	
Ramakanth et al.	2014	Approximate nearest neighbor and feature match	DIARETDB0	130	98.8	0.20
			DIARETDB1	89	98.1	0.20
			DRIVE	40	98.5	0.19
Proposed method		Maximum variance Method	STARE Began Singh Eye Hospital	81	99.81	110 ms
				100	98.47	131 ms

Table 6 Comparison of EX segmentation algorithm with literature-reviewed methods

Author name	Year	Algorithm	Database	No of images	SE (%)	SPE (%)	ACC (%)	Computation time(s)
Imani et al.	2016	Dynamic thresholding, Morphological processing, False positive removal	DIARETDB1 HEI-MED E-OPHTHA	89 169 82	89.01 81.26 80.32	99.93 99.81 99.83	NA	NA
Annunziata et al.	2016	Green channel homogenization Approximate exudates detection Exudates inpainting	STARE HRF	20 45	71.28 71.28	98.36 98.36	95.62 95.81	60
Naqvi et al.	2015	Scale Invariant Feature Transform (SIFT) k-means Clustering Visual Dictionaries SVM	STARE DR1	400 234	97.18 92.70	83.10 81.02	95.02 87.23	NA
Pereira et al.	2015	Normalization, Double thresholding, Ant colony optimization algorithm	HEI-MED	169	80.82	99.16	97.85	NA
Agurto et al.	2014	Optimal thresholding of instantaneous amplitude (IA) components extracted from multiple frequency scales	UTHSC SA MESSIDOR	652 400	99 100	76 70	83 82	12
Harangi et a l.	2014	Multiple active contours and region wise classification	DIARETDB1 HEI-MED	29 54	92 87	68 86	82 86	31
Zhang et al.	2014	Candidate extraction: Mathematical morphology	E-OPHTHA	47	96	89	–	35
Ali et al.	2013	Thresholding, Steerable and kirsch filter	HEI-MED	104	82.5	–	82.60	–
Proposed method		Inverse surface adaptive thresholding	STARE Began Singh Eye Hospital	81 100	98.72 96.63	89.58 92.56	99.13 98.34	0.76 0.65

Table 7 Comparison of MA detection algorithm with literature-reviewed methods

Author name	Year	Algorithm	Database	No of images	SE (%)	SPE (%)	ACC (%)	Computation time(S)
Seoud et al.	2016	Dynamic shape features	Messidor Erlangen CARA1006	1200 45 1006	93.9	50	–	98
Rosas-Romero et al.	2015	Reduction of non-uniform illumination and normalization, Selection of candidate based on shape and intensity	DIARETDB1 ROC	89 100	92.32 88.06	93.87 97.47	–	404.3 184.66
Adal et al.	2014	Scale-adapted blob analysis, local scale estimation, Scale-space features, Speeded up robust features, Radon-transform features	ROC UTHSC	100 380	81.08	92.31	–	–
Sopharak et al.	2013	Mathematical morphology Naive bayes classifier	Thammasat University Hospital	80	85.68	99.99	99.99	60
Lazar et al.	2013	Local rotating cross-section profile analysis	ROC	60	–	–	–	2
Zhang et al.	2010	Multi-scale correlation coefficients	ROC DIARETDB1	100 89	71.3	–	–	–
Akram et al.	2013	Morphological operation, Contrast normalization and filter banks, GMM, SVM, m-Mediods	DIARETDB0 DIARETDB1	130 89	98.64	99.69	99.40	2.93e-004 8.28e-004 3.17e-004
Tavakoli et al.	2013	Radon transform multi-overlapping windows	Mashhad Tehran ROC	120 5 22	94 100	75 70		660,665.20 ±80.368 580.37±33.814 41.66±9.128
Proposed method		Multi-agent approach	Began Singh Eye Hospital	100	99.82	98.13	99.67	0.19

Table 8 Comparison of HA segmentation algorithm with literature-reviewed methods

Author name	Year	Algorithm	Database	No of images	SE (%)	SPE (%)	ACC (%)	Computation time(S)
Hatanaka et al.	2008	Brightness correction	Own database	125	80	88	–	–
Grisan et al.	2007	Local thresholding, Pixel density	Own database	60	–	–	94	–
Zhang et al.	2005	Color normalization,two dimensional principal component analysis, SVM	Singapore National Eye Centre	30	–	–	–	–
Proposed method		Tobaggan segmentation	Began Singh Eye Hospital	100	90.02	88.43	93.21	0.28

Blood Vessels Detection

The preprocessing steps like low and high limit in CLAHE (Contrast Limited Adaptive Histogram Equalization) is used. The Gabor filter is swiveled in 12 different directions to get non-vessel and vessel pixels. The maximum response is computed and thresholding is applied to find small and large blood vessels. The Hysteresis thresholding is used to detect the final vessel map.

Optic Disc and Exudates detection

Localization of OD is an essential step in analysis of fundus image and to develop CAD (Computer Aided Diagnosis) tool for DR. OD center detection is necessary to decrease false positive rate in exudates detection (EXs). EXs is the white lesion present in the retina which is the early symptom for the diagnosis of DR. OD is detected using intensity variation algorithm and EXs is segmented using inverse surface adaptive thesholding algorithm.

Detection of Microaneurysms and Hemorrhages

Image enhancement techniques like median filter, correction of shade, modified Kirsch filter and Gaussian filter are used to suppress the noise and to highlight the image features. Pinpointing pixel, pixel exploration, region padding, region growing and region well-founded techniques are used to segment MAs efficiently. The entire image of retina is separated into non-overlapping segments of similar intensities. An algorithm of image re-sampling which converts an image to uneven grid is referred as Super-pixel based representation. The gradient magnitude is computed and toboggan segmentation is used to segment HAS.

Blood Vessel Removal

To enhance the BVs with orientation from 15° to 180° with the interval of 15°, line detection algorithm is used. The transformation of top hat is performed using the following equation:

$$T_b(f) = f \cdot b - f \tag{1}$$

where T_b (f) is the transformation of top-hat, b is the line-shaped element structuring, (•) is the closing operation and f is the image filtering [17]. BV elimination is performed to detect the presence of MAs and HAs more effectively.

Feature Vector Formation

According to the ETDRS, various lesions classification (i.e. white lesions and red lesions) can be preformed based on 7 characteristics which are shape, size, edge sharpness, roughness, depth, color and brightness [18].

In the proposed work, an attempt has been made to classify EXs, MAs and HAs. These three lesions seems with differentiable properties such as size, shape and color. Exudates are white in color, large in size, or with irregular shape. MAs are reddish in color, small in size with circular shape. HAs are large in size, reddish in color with irregular shape. The features such as area, perimeter, energy, orientation, mean, variance, SD, vessel diameter and vessel width are extracted from BVs. The features such as mean, variance, SD, skewness, covariance, median, area, perimeter, compactness ratio, eccentricity, mass deficiency coefficient, Shannon entropy, edge sharpness, equidistance, Euler number, orientation, contrast, homogeneity, correlation, energy, solidity, extend and aspect ratio are extracted from white and red lesions.

Table 9 Summary of data sets

Database	Images	Healthy	Unhealthy	FOV(°)	Resolution (pixel)
DRIVE	40	33	7	45	565 × 584
STARE	81	31	50	50	605 × 700
DIARETDB0	130	20	110	50	1500 × 1152
DIARETDB1	89	5	84	35	1500 × 1152
MESSIDOR	1200	546	654	45	2240 × 1488

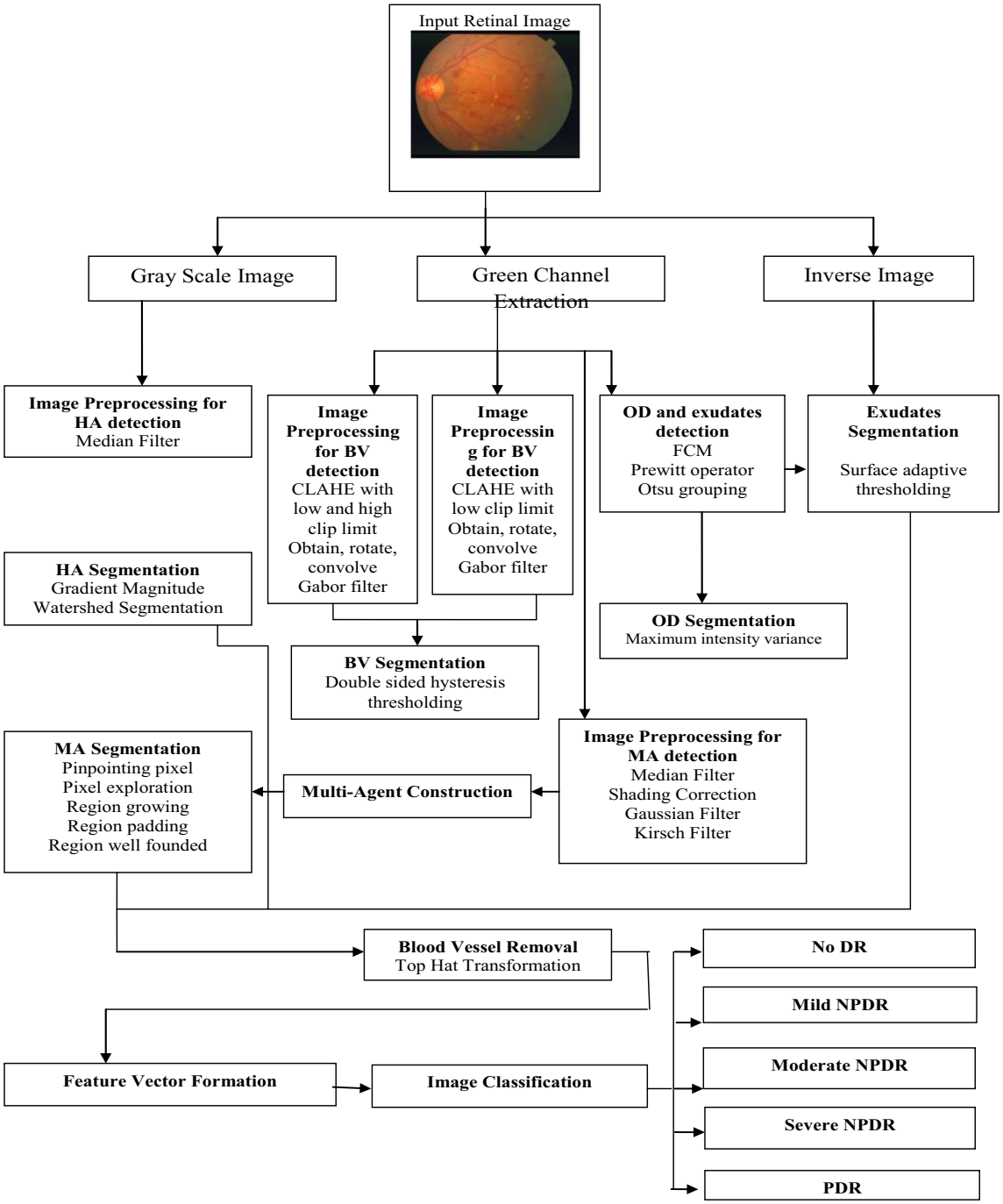

Fig. 2 Methodology for automated identification of DR

The statistical importance is examined using One-way test of ANOVA. Among the 55 features, mean, variance, standard deviation, area and perimeter are chosen from statistical test of ANOVA, and the chosen fifteen characteristics are employed for classification. Tables 10 and 11 show the extracted features and their corresponding range of minimum and maximum values in pixels for BVs, EXs, MAs and HAs.

Classification of DR

In the proposed work, two classifiers, namely NB [19] and SVM-RBF [20] are used to categorize images as abnormal or normal, and three classifiers, namely PRNN, RBFEF and RBFFN [21] have been employed to categorize the stages of DR. The images of retina are classified as normal image or DR affected image using appropriate tools based on their features.

Table 10 Names of Feature with characteristics of min-max and their ranges in Blood Vessels

S.No.	Feature Name	BVs(min-max) in pixels
1.	Area	317,916-2,558,463
2.	Perimeter	44,517-564,341
3.	Energy	0.4477-0.7018
4.	Orientation	−77,335 to −51
5.	Mean	−0.6927 to −0.4338
6.	Variance	0.2645 -0.6402
7.	Standard deviation	0.5142 - 0.8001
8.	Vessel diameter	2.0340 -2.6142
9.	Vessel width	2.0160 - 3.1365

The marked image are classified as abnormal or normal with the aid of NB, and SVM-RBF is graded with the severity of DR with neural network tools available in MATLAB software.

The DR affected retinal images are classified using the statistically significant features such as mean, variance, Standard Deviation(SD), area and perimeter (BVs, white lesions and red lesions). The NN classifiers like PRNN, RBFEF, and RBFFN comprises 3 three layers, which are hidden layer, input layer and output layers. For input layer fifteen nodes, 10 is set as hidden neurons, and 5 nodes are there for output layer which are normal image, mild NPDR affected image, moderate NPDR affected image, severe NPDR affected image and PDR affected image. Fifteen features are used for input layer with 100 images (20 are normal, 80 are abnormal), and the targets are set as abnormal and normal. Out of the 80 abnormal images, 20 are mild NPDR, 20 are moderate NPDR, 20 are severe NPDR and 20 are PDR.

Results and Discussion

The diagnosis of Diabetic Retinopathy performance is also analyzed quantitatively using various measures. The results of retinal landmark and lesion extraction from Indian Eye Database are given in Fig. 3. The images with various stages of DR are mentioned row-wise in Fig. 3a-e. The input retinal fundus image, detection of BVs, detection of center of OD, segmentation of EXs, HAs and MAs are given column-wise in Fig. 3f-k. Table 12 shows the comparative analysis of classification of DR with literature-reviewed methods. Bi-dimensional integrated index and empirical mode decomposition have been used for the growth of automated system of screening, and yielded SE of 86.25%, SPE of 91% and ACC of 88.63% respectively [5]F. Supervised classifiers like SVM, and PNN have been used to classify the severity in EXs-appeared image with SE of 98.68%, 96.64%, SPE of 100%, 98.46% and ACC of 97.89%, 94.76 respectively [6]. Differentiating normal and pathological

Table 11 Feature names with min-max characteristics and their ranges in EX and MA/HA

S. No	Feature Name	EXs(min-max) in pixels	MAs/HAs (min-max)in pixels
1.	Mean	0.000079-0.067135	0.00026-0.037405
2.	Variance	0.000079-0.062628	0.00026-0.036006
3.	Standard deviation	0.008908-0.250257	0.16114-0.18975
4.	Skewness	1108-40,433	2016-84,486
5.	Covariance	0.057551-6169.13634	0.83443-6405.5557
6.	Median	33-27,008	89-86,998
7.	Area	34-26,998	93-86,618
8.	Perimeter	24-2551	95-10,064
9.	Compactness ratio	0.024656-0.741765	0.01074-0.35779
10.	Eccentricity	0.28571-1.8	0.66667-1.84782
11.	Mass deficiency coefficient	0.028571-0.988502	0.86958-0.98896
12.	Shannon	0.001594-0.355141	0.01074-0.35779
13.	Edge Sharpness	0.421727-4.458253	0.00346-0.23026
14.	Equidistance	6.579524-185.40474	10.881-332.09255
15.	Euler number	1-46	−39 to 73
16.	Orientation	−260 to 669	−102 to 2157
17.	Contrast	0.00008-0.002279	0.000237 - 0.005539
18.	Homogeneity	0.99590054-1	0.99723-1
19.	Correlation	0.499957-0.961959	0.46224-0.95142
20.	Energy	0.869887-1	0.922562-1
21.	Solidity	1-7	1-8
22.	Extend	0.222453-1	0.43386-1
23.	Aspect ratio	0.45-2.062223	0.23021-0.94871

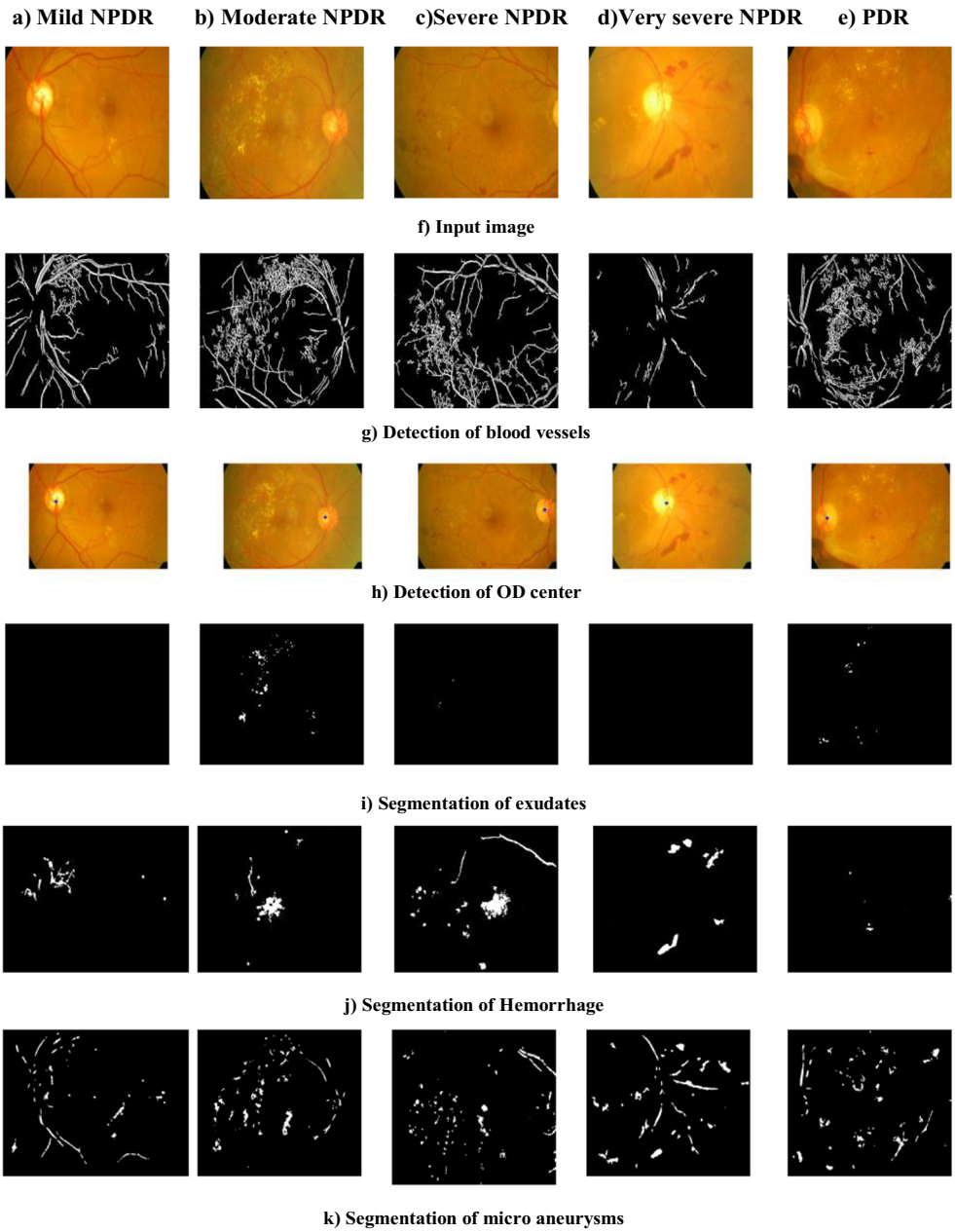

Fig. 3 Results of segmentation of Optic Disc, Exudates, Microaneurysms and Hemorrhages

retinal structures have been carried out by morphological component analysis and have yielded SE of 92.01%, SPE of 95.45% and ACC of 92.82% [7].

Decomposition of cartoon + texture, Hessian multi-scale analysis and variational segmentation have been used to segment lesions and appropriate binary classifiers are used to classify. Their method has achieved SE of 95-100% and SPE of 70% [8]. Two, three, four and five class classification of NPDR and PDR have been carried out by three different classifiers with thirteen features and have yielded SE of 95.26%, 100%, 96.27% and SPE of 88.33%, 100%, 96.08% respectively [9]. The mathematical morphology and SVM have been used for identification of lesion and classification. Their methods have showed.

ACC of 97.47% and 98.19% [10, 11]. In the proposed work, the system has yielded SE of 100%, SPE of 98.75%, and ACC of 95.24% and a computation time of 29 s. Among the reported results, the proposed classification algorithm is superior for SE and computation time.

Conclusion

Diabetic Retinopathy is the major cause of loss of vision worldwide. A Decision Suport System(DSS) to assist ophthalmologists for diagnosing DR has been developed. Image processing algorithms are used to segment retinal landmarks like OD and

Table 12 Comparative analysis of classification of DR with Literature reviewed methods

Author name	Year	Algorithm		Database	No of images	SE	SPE	ACC	Computation time
		Lesion detection	Classification						
Acharya et al. [5]	2016	Bi-dimensional empirical mode decomposition and integrated index	SVM-RBF	Kasturba medical college	800	86.25	91	88.63	50
Mahendran et al. [6]	2015	Exudates detection-Score computation	SVM PNN	Messidor	370	98.68 96.64	100 98.46	97.89 94.76	–
Imani et al. [7]	2015	Morphological component analysis	Statistical feature	Messidor	930	92.01	95.45	92.82	–
Figueiredo et al. [8]	2015	Wavelets, multiscale analysis Hessian matrix, cartoon texture image decomposition, variational image Segmentation, Threshold	Binary classifier	Retmarker	45,770	93 86 90 95-100	87 90 97 70	-`	–
Mookiah et al. [9]	2013	A-FIS histon, Thresholding, Morphology	SVM C4.5 PNN	Kasturba medical college	156	95.26 100 96.27	88.33 100 96.08	77.56 88.46 96.15	
Jerald jebakumar et al. [10]	2012	Image denoising, Gabor filter, Thresholding, Morphological operation	SVM	Began Singh Eye Hospital	90	–	–	97.47	–
Madheswaran et al. [11]	2012	Block processing, Thresholding, Pixel flushing, morphological operation	SVM Bright Dark	Began Singh Eye Hospital	90	96.61 88.54	98.31 98.23	98.19 97.51	–
Proposed method		Hybrid approach	SVM-RBF PRNN	Began Singh Eye Hospital	100	95 100	98.75 98.75	98 99	28 29

BVs, and they are removed for further processing because they invariably appear in segmented output of white and red lesions. MAs, HAs and EXs have been segmented with novel segmentation algorithms like muti-agent approach, toboggan segmentation and inverse surface adpative thresholding. The machine learning techniques are employed to categorize DR images into abnormal/normal with SVM-RBF, and the results are compared with existing NB. Again, it has been classified into normal, mild Non Proliferative Diabetic Retinopathy, severe Non Proliferative Diabetic Retinopathy, moderate Non Proliferative Diabetic Retinopathy, and Proliferative Diabetic Retinopathy using PRNN, and the outputs are compared with RBFEF and RBFFN. The summary of the performance evaluation of diagnosis of DR is tabulated in Table 13. The results obtained for the retinal images are compared with ground truth images. The performance measures such as SE, SPE, and ACC values obtained are {89.08%, 90.32%, 98.19%}, {−,-,98.47%},{96.63%, 92.56%, 98.34%},{99.82%, 98.13%, 99.67%},{90.02%, 88.43%, 93.21%},{95%, 98.75%, 98%},{100%, 98.75%, 95.24%} for segmentation of blood vessels, Optic Disc, Exudates, Microaneurysms, Hemorrhages, 2 class classification and 5 class classification respectively.

This screening system does not require any maintenance by doctors, patients or medical personals. In future, it has been planned to use spectral domain optical coherence tomography images to detect retinal lesions and better classifiers to classify various stages of DR.

Table 13 Summary of performance evaluation towards the diagnosis of DR

Retinal landmark/ lesion	Algorithm used	SE (%)	SPE (%)	ACC (%)	Computation time
Blood vessel	Gabor double-sided hysteresis thresholding	89.08	90.32	98.19	49.92 ms
Optic disc	Maximum intensity variation	–	–	98.47	131 ms
Exudates	Inverse surface adaptive thresholding	96.63	92.56	98.34	0.65 ms
Microaneurysms	Multi-agent approach	99.82	98.13	99.67	0.19 s
Hemorrhages	Toboggan segmentation	90.02	88.43	93.21	0.28 s
2 class classification	SVM-RBF	95	98.75	98	28 s
5 class classification	PRNN	100	98.75	95.24	29 s

Compliance with ethical standards

Conflict of Interest This paper has not communicated anywhere till this moment, now only it is communicated to your esteemed journal for the publication with the knowledge of all co-authors.

Ethical approval This article does not contain any studies with human participants or animals performed by any of the authors.

References

1. Zaki, W. M. D. W., Zulkifley, M. A., Hussain, A., Halim, W. H. W. A., Mustafa, N. B. A., and Ting, L. S., Diabetic retinopathy assessment: Towards an automated system. Biomedical Signal Processing and Control 24:72–82, 2016.
2. Olson, J. L., Asadi-Zeydabadi, M., and Tagg, R., Theoretical estimation of retinal oxygenation in chronic diabetic retinopathy. Computers in Biology and Medicine 58:154–162, 2015.
3. Yun, W. L., Acharya, U. R., Venkatesh, Y. V., Chee, C., Min, L. C., and Ng, E. Y. K., Identification of different stages of diabetic retinopathy using retinal optical images. Information Sciences 178(1): 106–121, 2008.
4. Akram, M. U., Khalid, S., and Khan, S. A., Identification and classification of microaneurysms for early detection of diabetic retinopathy. Pattern Recognition 46(1):107–116, 2013.
5. Acharya, U. R., Mookiah, M. R. K., Koh, J. E., Tan, J. H., Bhandary, S. V., Rao, A. K., Fujita, H., Hagiwara, Y., Chua, C. K., and Laude, A., Automated screening system for retinal health using bi-dimensional empirical mode decomposition and integrated index. Computers in biology and medicine 75:54–62, 2016.
6. Mahendran, G., and Dhanasekaran, R., Investigation of the severity level of diabetic retinopathy using supervised classifier algorithms. Computers & Electrical Engineering 45:312–323, 2015.
7. Imani, E., Pourreza, H. R., and Banaee, T., Fully automated diabetic retinopathy screening using morphological component analysis. Computerized Medical Imaging and Graphics 43:78–88, 2015.
8. Figueiredo, I. N., Kumar, S., Oliveira, C. M., Ramos, J. D., and Engquist, B., Automated lesion detectors in retinal fundus images. Computers in biology and medicine 66:47–65, 2015.
9. Mookiah, M. R. K., Acharya, U. R., Martis, R. J., Chua, C. K., Lim, C. M., Ng, E. Y. K., and Laude, A., Evolutionary algorithm based classifier parameter tuning for automatic diabetic retinopathy grading: A hybrid feature extraction approach. Knowledge-based systems 39:9–22, 2013.
10. Kumar, S. J. J., and Madheswaran, M., An improved medical decision support system to identify the diabetic retinopathy using fundus images. Journal of medical systems 36(6):3573–3581, 2012.
11. Madheswaran, M., and Kumar, S. J. J., An Improved Medical Decision Support System To Grading The Diabetic Retinopathy Using Fundus Images. ICTACT Journal On Image and Video Processing 3(02):502–510, 2012.
12. Staal, J., Abràmoff, M. D., Niemeijer, M., Viergever, M. A., and Van Ginneken, B., Ridge-Based Vessel Segmentation in Color Images of the Retina. IEEE Transactions on Medical Imaging 23(4):501–509, 2004.
13. Hoover, A. D., Kouznetsova, V., and Goldbaum, M., Locating blood vessels in retinal images by piecewise threshold probing of a matched filter response. IEEE Transactions on Medical Imaging 19(3):203–210, 2000.
14. Decencière, E., Zhang, X., Cazuguel, G., Lay, B., Cochener, B., Trone, C., Gain, P., Ordonez, R., Massin, P., Erginay, A., Charton, B., and Klein, J.-C., Feedback on a publicly distributed database: the Messidor database. Image Analysis & Stereology 33(3):231–234, 2014.
15. Kauppi, T, Kalesnykiene, V, Kamarainen, JK, Lensu, L, Sorri, I, Uusitalo, H, Kälviäinen, H & Pietilä, J 2006, 'DIARETDB0: Evaluation database and methodology for diabetic retinopathy algorithms', Machine Vision and Pattern Recognition Research Group, Lappeenranta University of Technology, Finland, pp.134.
16. Kauppi, T, Kalesnykiene, V, Kamarainen, J.-K, Lensu, L, Sorri, I, Raninen A, Voutilainen R, Uusitalo, H, Kälviäinen, H & Pietilä, J 2007, 'DIARETDB1 diabetic retinopathy database and evaluation protocol, in proceedings of the eleventh conference on Medical Image Understanding and Analysis, pp.1-10.
17. El Abbadi, N. K., and Al Saadi, E. H., Blood vessels extraction using Mathematical Morphology. Journal of Computer Science 9(10):1389–1395, 2013.
18. Saleh, M. D., and Eswaran, C., An automated decision-support system for non-proliferative diabetic retinopathy disease based on MAs and HAs detection. Computer methods and programs in biomedicine 108(1):186–196, 2012.
19. Dua, S., Acharya, U. R., Chowriappa, P., and Sree, S. V., Wavelet basedenergy features for glaucomatous image classification. IEEE transactions on information technology in biomedicine 16(1):80–87, 2012.
20. Acharya, U. R., Mookiah, M. R. K., Koh, J. E., Tan, J. H., Noronha, K., Bhandary, S. V., Rao, A. K., Hagiwara, Y., Chua, C. K., and Laude, A., Novel risk index for the identification of age-related macular degeneration using radon transform and DWT features. Computers in biology and medicine 73:131–140, 2016.
21. Santhi, D., Manimegalai, D., Parvathi, S., and Karkuzhali, S., Segmentation and classification of bright lesions to diagnose diabetic retinopathy in retinal images. Biomedical Engineering/ Biomedizinische Technik 61(4):443–453, 2016.